AFRL-RX-WP-JA-2017-0325

TEMPORAL DYNAMICS OF TWO-BEAM COUPLING AND THE ORIGIN OF COMPENSATION PHOTOREFRACTIVE GRATINGS IN $Sn_2P_2S_6$:Sb (POSTPRINT)

Yaroslav Skrypka, Alexandr Shumelyuk, and Serguey Odoulov
National Academy of Sciences

Sergey Basun
Azimuth Corporation

Dean R. Evans
AFRL/RX

16 March 2017
Interim Report

(STINFO COPY)

AIR FORCE RESEARCH LABORATORY
MATERIALS AND MANUFACTURING DIRECTORATE
WRIGHT-PATTERSON AIR FORCE BASE, OH 45433-7750
AIR FORCE MATERIEL COMMAND
UNITED STATES AIR FORCE

REPORT DOCUMENTATION PAGE

Form Approved
OMB No. 0704-0188

1. REPORT DATE *(DD-MM-YY)*	2. REPORT TYPE	3. DATES COVERED *(From - To)*
16 March 2017	Interim	23 August 2016 – 16 February 2017

4. TITLE AND SUBTITLE

TEMPORAL DYNAMICS OF TWO-BEAM COUPLING AND THE ORIGIN OF COMPENSATION PHOTOREFRACTIVE GRATINGS IN $Sn_2P_2S_6$:Sb (POSTPRINT)

5a. CONTRACT NUMBER
FA8650-16-F-5419

5b. GRANT NUMBER

5c. PROGRAM ELEMENT NUMBER
62102F

6. AUTHOR(S)

1) Yaroslav Skrypka, Alexandr Shumelyuk, and Serguey Odoulov - NAS

2) Sergey Basun – Azimuth Corporation

(continued on page 2)

5d. PROJECT NUMBER
4348

5e. TASK NUMBER

5f. WORK UNIT NUMBER
X14W

7. PERFORMING ORGANIZATION NAME(S) AND ADDRESS(ES)

1) Institute of Physics
National Academy of Sciences
03 650 Kyiv, Ukraine

2) Azimuth Corporation
4027 Colonel Glenn Hwy
Beavercreek, OH 45431

(continued on page 2)

8. PERFORMING ORGANIZATION REPORT NUMBER

9. SPONSORING/MONITORING AGENCY NAME(S) AND ADDRESS(ES)

Air Force Research Laboratory
Materials and Manufacturing Directorate
Wright-Patterson Air Force Base, OH 45433-7750
Air Force Materiel Command
United States Air Force

10. SPONSORING/MONITORING AGENCY ACRONYM(S)
AFRL/RXAP

11. SPONSORING/MONITORING AGENCY REPORT NUMBER(S)
AFRL-RX-WP-JA-2017-0325

12. DISTRIBUTION/AVAILABILITY STATEMENT
Distribution Statement A. Approved for public release: distribution unlimited.

13. SUPPLEMENTARY NOTES
PA Case Number: 88ABW-2017-1063; Clearance Date: 16 Mar 2017. This document contains color. Journal article published in Optical Materials Express, Vol. 7, No. 4, 1 Apr 2017. © 2017 Optical Society of America. The U.S. Government is joint author of the work and has the right to use, modify, reproduce, release, perform, display, or disclose the work.
The final publication is available at https://doi.org/10.1364/OME.7.001414

14. ABSTRACT *(Maximum 200 words)*

Photorefractive effect in $Sn_2P_2S_6$ (SPS) is caused by a spatial redistribution of both positively charged and negatively charged carriers, which leads to the formation of two out-of-phase space charge gratings that partially compensate each other in the steady state. The unusual intensity dependence of the compensation grating buildup time is reported in this article for antimony doped SPS; it is explained by the thermal excitation of electrons into conduction band from the optically recharged $Sb^{3+} \rightarrow Sb^{2+}$ impurity ions.

15. SUBJECT TERMS

Photorefractive materials; Nonlinear wave mixing; Optical nonlinearities of condensed matter; Spectroscopy, four-wave mixing

16. SECURITY CLASSIFICATION OF:			17. LIMITATION OF ABSTRACT:	18. NUMBER OF PAGES	19a. NAME OF RESPONSIBLE PERSON (Monitor)
a. REPORT	b. ABSTRACT	c. THIS PAGE			Timothy White
Unclassified	Unclassified	Unclassified	SAR	13	19b. TELEPHONE NUMBER *(Include Area Code)* (937) 255-9551

REPORT DOCUMENTATION PAGE Cont'd

6. AUTHOR(S)

3) Dean R. Evans - AFRL/RX

7. PERFORMING ORGANIZATION NAME(S) AND ADDRESS(ES)

3) AFRL/RX, Wright-Patterson AFB,
Dayton, OH 45433

Research Article | Vol. 7, No. 4 | 1 Apr 2017 | OPTICAL MATERIALS EXPRESS 1414

Optical Materials EXPRESS

Temporal dynamics of two-beam coupling and the origin of compensation photorefractive gratings in $Sn_2P_2S_6$:Sb

YAROSLAV SKRYPKA,[1] ALEXANDR SHUMELYUK,[1] SERGUEY ODOULOV,[1,*] SERGEY BASUN,[2,3] AND DEAN R. EVANS[3]

[1] *Institute of Physics, National Academy of Sciences, 03 650 Kyiv, Ukraine*
[2] *Azimuth Corporation, 4027 Colonel Glenn Highway, Beavercreek, OH 45431, USA*
[3] *Air Force Research Laboratory, Materials and Manufacturing Directorate, Wright Patterson AFB, Dayton, OH 45433, USA*
[*] *odoulov@iop.kiev.ua*
http://www.iop.kiev.ua/ prc/

Abstract: Photorefractive effect in $Sn_2P_2S_6$ (SPS) is caused by a spatial redistribution of both positively charged and negatively charged carriers, which leads to the formation of two out-of-phase space charge gratings that partially compensate each other in the steady state. The unusual intensity dependence of the compensation grating buildup time is reported in this article for antimony doped SPS; it is explained by the thermal excitation of electrons into conduction band from the optically recharged $Sb^{3+} \rightarrow Sb^{2+}$ impurity ions.

OCIS codes: (160.5320) Photorefractive materials; (190.4223) Nonlinear wave mixing; (190.4720) Optical nonlinearities of condensed matter; (300.6290) Spectroscopy, four-wave mixing.

References and links

1. S. Odoulov, A. Shumelyuk, U. Hellwig, R. Rupp, A. Grabar, and I. Stoyka, "Photorefraction in tin hypothiodiphosphate in the near infrared," J. Opt. Soc. Am. B **13**(10), 2352–2360 (1996).
2. S. Odoulov, A. Shumelyuk, U. Hellwig, R. Rupp, A. Grabar, and I. Stoyka, "Photorefractive beam coupling in tin hypothiodiphosphate in the near infrared," Opt. Lett. **21**(10), 752–754 (1996).
3. M. Miteva and L. Nikolova, "Oscillating behavior of diffracted light on uniform illumination of holograms in photorefractive $Bi_{12}TiO_{20}$ crystals," Opt. Commun. **67**(3), 192–194 (1988).
4. S. Zhivkova and M. Miteva, "Holographic recording in photorefractive crystals with simultaneous electron-hole transport and two active centers," Appl. Phys. **68**(7), 3099–3103 (1990).
5. V. Jerez, I. de Oliveira, and J. Frejlich, "Optical recording mechanisms in undoped titanosillenite crystals," Appl. Phys. **109**, 024901 (2011).
6. A. Donnermeyer, H. Vogt, and E. Krätzig, "Complementary gratings due to electron and hole conductivity in aluminium-doped bismuth titanium oxide crystals," Phys. Stat. Sol. (a) **200**(2), 451–256 (2003).
7. A. Donnermeyer and E. Krätzig, "Influence of light intensity and crystal temperature on photorefractive charge-compensation processes in Al-doped $Bi_{12}TiO_{20}$ crystals," Phys. Stat. Sol. (a) **201**(3), 1257–1259 (2004).
8. A. Grabar, M. Jazbinsek, A. Shumelyuk, Yu. Vysochanskii, G. Montemezzani, and P. Günter, "Photorefractive effects in $Sn_2P_2S_6$," in *Photorefractive Materials and Their Applications 2: Materials*, P. Günter and J.-P. Huignard, eds. Vol. 114 of Springer Series in Optical Sciences (Springer, 2007), pp. 327 – 362.
9. J. J. Amodei and D. L. Staebler, "Holographic pattern fixing in electrooptic crystals," Appl. Phys. Lett. **18**(12), 540–542 (1971).
10. G. Montemezzani, M. Zgonik, and P. Günter, "Photorefractive charge compensation at elevated temperatures and application to $KNbO_3$," J. Opt. Soc. Am. B **10**(2), 171–185 (1993).
11. A. Shumelyuk, A. Hryhorashchuk, S. Odoulov, and D. R. Evans, "Transient gain enhancement in photorefractive crystals with two types of movable charge carrier," Opt. Lett. **32**(14), 1959–1961 (2007).
12. A. Shumelyuk, A. Hryhorashchuk, and S. Odoulov, "Coherent optical oscillator with periodic zero-Pi phase modulation," Phys. Rev. A **72**, 023819 (2005).
13. A. Shumelyuk, A. Hryhorashchuk, and S. Odoulov, "Optical multivibrator with ferroelectric $Sn_2P_2S_6$," Ferroelectrics, **348**(1), 19–24 (2007).
14. D R. Evans, A. Shumelyuk, G. Cook, and S. Odoulov, "Secondary photorefractive centers in $Sn_2P_2S_6$:Sb crystals," Opt. Lett. **36**(4), 454–456 (2011).
15. J. Strait and A. M. Glass, "Time-resolved photorefractive four-wave mixing in semiconductor materials," J. Opt. Soc. Am. B **3**(2) 342–344 (1986).

#286133 https://doi.org/10.1364/OME.7.001414
Journal © 2017 Received 6 Feb 2017; accepted 8 Mar 2017; published 29 Mar 2017

Optical Materials EXPRESS

16. I. V. Kedyk P. Mathey G. Gadret A. A. Grabar, K. V. Fedyo I. M. Stoika I. P. Prits, and Yu. M. Vysochanskii, "Investigation of the dielectric, optical and photorefractive properties of Sb-doped $Sn_2P_2S_6$ crystals," Appl. Phys. B **92**(4), 549–554 (2008).
17. T. Bach, M, Jazbinsek, G. Montemezzani, P. Günter, A. A. Grabar, and Y M. Vysochanskii, "Tailoring of infrared photorefractive properties of $Sn_2P_2S_6$ crystals by Te and Sb doping," J. Opt. Soc. Am. B **24**(7), 1535–1541 (2007).
18. B. Sturman, P. Mathey, H. R. Jauslin, S. Odoulov, and A. Shumelyuk, "Modeling of the photorefractive nonlinear response in $Sn_2P_2S_6$ crystals," J. Opt. Soc. Am. B **24**(6), 1301–1309 (2007).
19. A.T. Brant, L.E. Halliburton, S.A. Basun, A.A. Grabar, S.G. Odoulov, A. Shumelyuk, N.C. Giles, and D.R. Evans, "Photoinduced EPR study of Sb^{2+} ions in photorefractive $Sn_2P_2S_6$ crystals," Phys. Rev. B **86**, 134109 (2012).
20. Y. Skrypka, A. Shumelyuk, S, Odoulov, S. Basun, and D. Evans, "Light induced absorption and optical sensitizing of $Sn_2P_2S_6$:Sb," Opt. Commun. **356**, 208–211 (2015).
21. S. Basun, L. E. Halliburton, and D. R. Evans, "Hyperbolic decay of photo-created Sb^{2+} ions in $Sn_2P_2S_6$ crystals detected with electron paramagnetic resonance," Appl. Phys. Lett. **110**, 052903 (2017).
22. R. V. Gamernyk, Yu. P. Gnatenko, P. M. Bukivsij, P. A. Skubenko, and V. Yu. Slivka, "Optical and photoelectric spectroscopy of photorefractive $Sn_2P_2S_6$ crystals," J. Phys.: Condens. Matter **18**(23), 5323–5331 (2006).
23. S. A. Basun and D. R. Evans, "Identification of the specific Fe centers and associated defects of structure responsible for enhanced dynamic holography in photorefractive $KNbO_3$:Fe," Phys. Rev. B **93** 094102 (2016).
24. A .T. Brant, L. E. Halliburton, N. C. Giles, S. A. Basun, A. A. Grabar, and D. R. Evans, "Intrinsic small polarons (Sn^{3+} ions) in photorefractive $Sn_2P_2S_6$ crystals," J. Phys.: Condens. Matter **25**, 205501 (2013).
25. J. Feinberg, D. Heiman, A. R. Tanguay, Jr., and R. Hellwarth, "Photorefractive effects and light-induced charge migration in barium titanate," Appl. Phys. **51**(3), 1297–1305 (1980).
26. K. Shcherbin, "High photorefractive gain at counterpropagating geometry in CdTe:Ge at 1.064 μm and 1.55 μm," Appl. Opt. **48**(2), 371–374 (2009).
27. Boris I. Sturman, "Space-Charge Wave Effects in Photorefractive Materials," in *Photorefractive Materials and Their Applications 1: Materials*, P. Günter and J.-P. Huignard, eds. Vol. 113 of Springer Series in Optical Sciences (Springer, 2006), pp. 119–162.

1. Introduction

Tin Hypothiodiphosphate ($Sn_2P_2S_6$, SPS) possesses impressive optical nonlinearities, especially a pronounced photorefractive effect in the red and near infrared spectral domains [1, 2]. From the first publications on photorefractive gratings recording with Nd^{3+} laser light (λ = 1.06 μm) in SPS it is known that quite fast amplification of a signal wave (in millisecond range) is followed by much slower (up to few minutes) decrease of its intensity until the certain steady state level is reached. A similar type of transient beam coupling has been reported earlier for sillenite crystals [3–7]; it was detected later in several doped SPS crystals (see, e.g., [8]). "Close relatives" of this effect are the thermal fixing process first observed in $LiNbO_3$ [9] and charge compensation at elevated temperatures first observed in $KNbO_3$ [10]. The formation of two complementary gratings in $Sn_2P_2S_6$ has been successfully used for transient gain enhancement [11] and for design of a coherent optical oscillator with particular temporal dynamics, "optical multivibrator" [12, 13].

Such temporal dynamics of two-beam coupling with a transient peak is explained by the presence of two types of movable charge carriers, holes and electrons. They both contribute to the formation of the space charge grating, but their particular contributions are exactly out-of-phase and tend to compensate each other. The necessary condition to observe transient coupling is a considerable difference of the characteristic build-up times τ_f and τ_s of the two contributions (subscripts f and s for fast and slow, respectively), which is related in part to a pronounced difference of the electron conductivity from the hole conductivity.

Practically in all cases mentioned in [1–8] the fast grating is developed by the optically excited charge carriers, while the compensation grating appears because of a redistribution of the thermally excited (optically inactive) carriers of opposite sign. This conclusion follows from the independence of the characteristic decay time of compensation grating τ_s of the recording (erasing) wave intensity (see, e.g., [7, 8]). The characteristic time of the fast grating τ_f depends on the dielectric relaxation time and is therefore inversely proportional to the sample conductivity and light intensity.

An atypical behavior of the compensation grating that consists of an intensity dependence of the slow grating characteristic decay time is reported in this paper for antimony doped SPS

Optical Materials EXPRESS

crystals. This particularity may be attributed to the thermal excitation of electrons from the optically populated impurity level Sb^{3+}/Sb^{2+} located within the bandgap close to the conduction band. The excessive density of free electrons in the conduction band being in quasiequilibrium with optically recharged antimony ions (Sb^{2+}) is linearly dependent on recording (erasing) light intensity. The free-electron component of the dielectric relaxation time τ_{di}^{e} has therefore a part which is inversely proportional to the intensity of light, thus affecting the slow component characteristic time τ_s.

We describe in this article two-beam coupling dynamics in SPS:Sb with the aim to characterize the crystal and identify the origin of the unusual behavior of the compensation grating.

2. Experimental results

The $Sn_2P_2S_6$ crystals studied in the experiment were grown in Uzhgorod National University, Ukraine, by a chemical vapor transport technique. All samples have been cut along the crystallographic axes, and their xy-faces were optically finished. The main part of the data shown below was obtained with 1% antimony doped sample K33 (6.0 x 4.5 x 8.0 mm^3), while some data were measured using another SPS:Sb(1%) sample K24 (2.0 x 3.5 x 2.4 mm^3). The results obtained for SPS:Sb were compared with the data measured in this work for nominally undoped Type I SPS [8] (9.0 x 4.5 x 9.0 mm^3). Two-beam coupling was studied in a standard experimental set-up. The copropagating pump and signal beams from the same He-Ne laser impinged upon the SPS sample in the xz-plane, with their bisector aligned along the sample z-axis; the transmitted signal beam was directed to the detector.

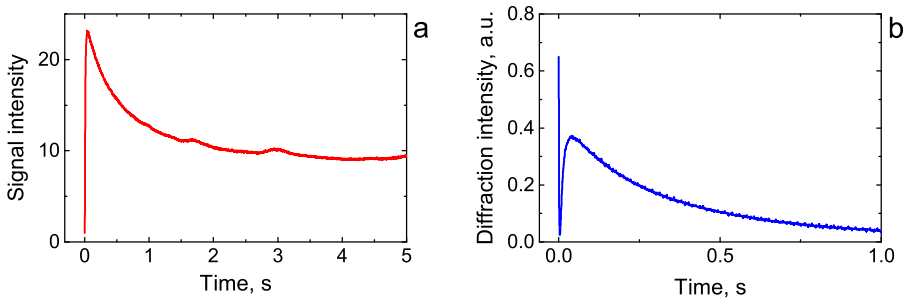

Fig. 1. Temporal dynamics of (a) two-beam coupling and (b) grating erasure in SPS:Sb sample K33. The output intensity of signal beam I_s in (a) is normalized to its initial value in the absence of the pump wave I_s^0. The diffraction efficiency in (b) is normalized to its saturation value. At $t = 0$ the signal wave is switched on in panel (a) and switched off in panel (b). The two recording waves from the He-Ne laser impinge upon the z-cut sample symmetrically in the xz-plane and are both y-polarized. The intensities of the signal and pump waves are 2 mW/cm^2 and 2 W/cm^2, respectively, and the grating spacing is 8 μm.

Figure 1(a) shows an example of the temporal dynamics of the amplified signal wave intensity for SPS:Sb. The input signal wave with the intensity I_s^0, which is much weaker than the pump intensity I_p, is switched-on at the moment $t = 0$. In the particular case shown, the output intensity of the signal wave increases 23 times within a few milliseconds and then a compensation grating develops during a few seconds resulting in a steady-state gain that is roughly half of its peak value. To reduce the coupling strength and remain well within the undepleted pump conditions the polarization of the two interacting waves was chosen to be normal to the interaction plane. A Pockels coefficient r_{221} which is roughly two times smaller than the largest coefficient for SPS crystal (r_{111}) defines the maximum two-beam coupling gain in this case. It should be mentioned that just before measuring the dynamics of two-beam coupling similar to Fig. 1(a), the sample was preexposed to a strong light wave to optically sensitize it; this process is described

Optical Materials EXPRESS

in reference [14]. When measuring the intensity dependences of the characteristic times, the intensity of preexposure was always the same as the intensity of the pump wave.

The presence of two space charge gratings manifests itself also in the temporal dynamics of the optical erasure of the recorded grating (Fig. 1(b)). If the input signal wave is terminated abruptly at $t = 0$, the interference pattern that records the grating no longer exists and the grating starts to decay. At $t > 0$ the detector monitors a part of the incident wave intensity which is diffracted from the grating in the direction of the signal wave. It can be seen that the diffracted signal drops quickly to zero and then increases reaching a maximum value and finally vanishes. This behavior has been explained in [1] as follows. The grating resulting from the fast recording process in Fig. 1(a) decays more quickly than the compensation grating. At a certain point the amplitudes of the two out-of-phase gratings become equal, which is when full compensation occurs, and the diffracted intensity goes to zero. As time increases, both contributions to the grating continue to decay with their own characteristic times; at this time interval the amplitude of the compensation grating is greater and contributes more to the diffracted signal. A maximum of the diffraction is reached when the amplitude of the fast grating is already small compared to that of compensation grating; for longer times we observe only a decrease of the diffracted intensity.

This interpretation is supported by an independent experiment, which proves that the diffracted wave phase changes to π at the moment when its intensity passes zero value (see Fig. 1(b)). Images of the fringe pattern formed at the output face of the sample by the transmitted readout (pump) wave and the diffracted wave have been taken before and after the moment of exact compensation. The obvious inversion of fringe contrast has been detected, thus proving that the diffraction occurs from the complementary gratings which are shifted exactly by half a period.

The diffraction efficiency of a grating, being proportional to the square of the index modulation, diminishes two times faster than the signal intensity when two interacting waves are present at the crystal input face (see, e.g., [15]. This can be clearly seen from a comparison of panels (a) and (b) in Fig. 1 (note that the time scales in (a) and (b) are not the same).

The two-beam coupling that results in amplification of the signal wave at the expense of the pump wave intensity is usually characterized by the gain factor $\Gamma \simeq -(1/\ell)\ln(I_s/I_s^0)$. In the considered case of SPS:Sb the gain factor has two components, fast and slow, given by:

$$\Gamma(t) = \Gamma_f\left[1 - \exp(-t/\tau_f)\right] - \Gamma_s\left[1 - \exp(-t/\tau_s)\right]. \quad (1)$$

By fitting Eq. (1) to the data shown in Fig. 1(a) the characteristic times τ_f and τ_s can be extracted. Taking similar measurements under different experimental conditions (light intensity, temperature, grating spatial frequency, etc.), a complete characterization of the beam coupling temporal dynamics can be accomplished.

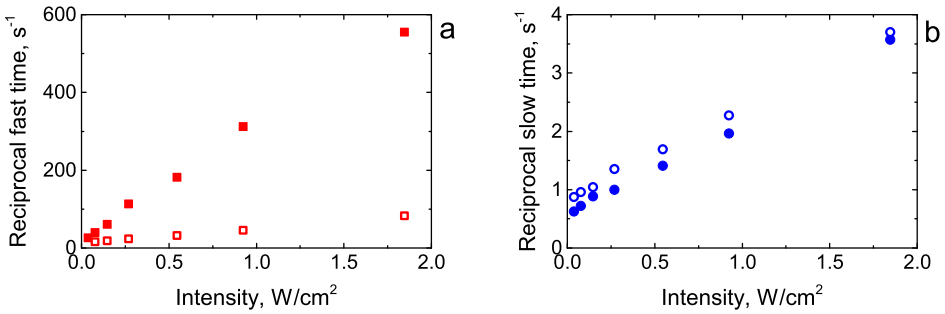

Fig. 2. Intensity dependences of reciprocal (a) fast and (b) slow times at ambient temperature for grating spacing 8 μm (filled symbols) and 1.0 μm (open symbols) for K33 SPS:Sb.

Optical Materials EXPRESS

Figure 2 shows the intensity dependences of τ_f and τ_s for two different grating spacings, 8 μm and 1 μm. The decrease of the both fast and slow grating lifetimes with the increasing I is evident (shown as a rise in reciprocal time). Within the intensity range from zero to 2 W/cm^2, a relative change of τ_f is greater for larger grating spacings; the opposite is true for τ_s. The characteristic time of the slow grating is nearly independent of grating spacing, but it does depend on the recording light intensity, which is contrary to that of nominally undoped SPS [8].

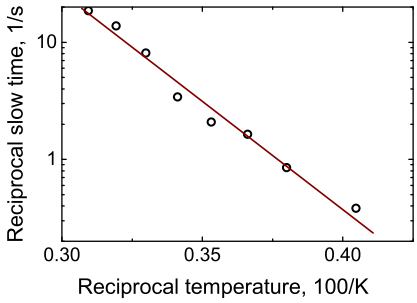

Fig. 3. Arrhenius plot for the reciprocal slow time measured with sample K24; grating spacing Λ = 6 μm, light intensity I = 0.4 W/cm^2.

Using a Peltier element the temperature of the sample could be controlled over the range from -25 to +50°C. The temperature dependence of τ_s was measured within this range and an Arrhenius plot for the slow grating recording time is shown in Fig. 3. The activation energy for formation of the compensation grating extracted from this plot is $\Delta E \simeq 0.42$ eV. Similar measurements with different light intensities up to 2 W/cm^2 did not show any regular intensity dependence for ΔE that remained within a range (0.44 ± 0.02) eV. The data for ΔE obtained from the temperature dependences of grating optical erasure (grating lifetime) are also in close agreement.

Figure 4 shows the spatial frequency dependences of the reciprocal times $1/\tau_f$ and $1/\tau_s$ for antimony doped SPS. With the same experimental set-up we measured similar dependences for a nominally undoped SPS crystal to get a reference for comparison. All these measurements lead to several qualitative and quantitative conclusions. One general conclusion is the confirmation of the transport lengths ratio: in the antimony doped crystal the Debye screening length is smaller than the diffusion length. This is a general rule for all doped and nominally undoped SPS crystals (including SPS:Sb [16]) with only one exception: the diffusion length is smaller than the Debye screening length in the so called "modified" or "brown" SPS crystal [16, 17]. It can be stated also, that the values of the fast grating times τ_f are very close for nominally undoped and antimony doped crystals, while τ_s may differ by several orders of magnitude for these crystals depending on the grating spacing. The slow grating time τ_s is distinguishable in SPS:Sb by its very weak dependence on grating spatial frequency.

From the comparison with theory for two-beam coupling in crystals with compensation gratings [18], it is possible to evaluate the characteristic transport lengths and get estimates for the effective hole trap density and free electron density. The relationship between characteristic time τ_s and grating spatial frequency K was derived in [18] within the approximation of compensating charges excited only thermally and is therefore unapplicable in our case. This approximation does not affect, however, the relationship between τ_f and K because the fast grating saturates well before the slow grating develops in full ($\tau_f \ll \tau_s$).

The dashed gray lines and solid red line in Fig. 4 show the results of the best fits of the measured characteristic relaxation times $\tau_{f,s}$ with calculated grating spacing dependences (given by Eqs. (10) of publication [18]). The details of characterization of nominally undoped crystals will be a topic of a separate publication, here we intend to compare macroscopic parameters for photoexcited holes such as dielectric relaxation time $\tau_{di}^h = \epsilon\epsilon_0/\sigma^h$, Debye screening length

Optical Materials EXPRESS

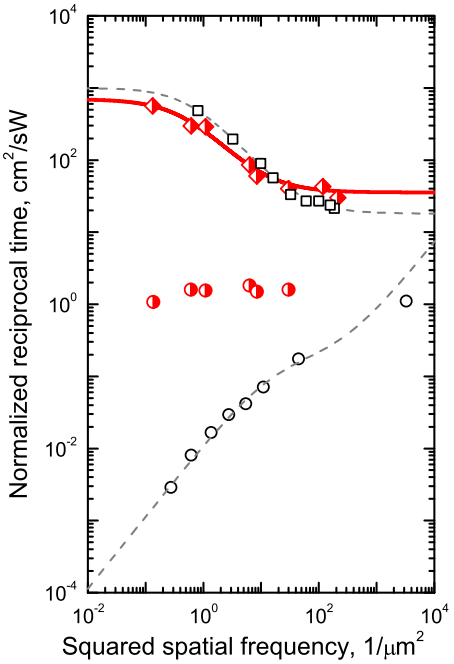

Fig. 4. Grating-spacing dependence of the reciprocal characteristic decay times normalized to the total intensity of two recording beams. Squares/diamonds and circles mark τ_f and τ_s, respectively. Half-filled (red) symbols are used for the antimony doped sample K33, while open symbols denote the nominally undoped reference sample. The lifetime for the compensation grating in the undoped sample is measured with I = 3 W/cm^2. Dashed and solid lines are the best fits of theoretical dependences as explained in text.

$\ell_s^h = \sqrt{\epsilon\epsilon_0 k_B T / N_{eff}^h e^2}$, and diffusion length $\ell_D^h = \sqrt{\mu\tau_c k_B T/e}$ (with low frequency dielectric susceptibility ϵ, total hole conductivity σ^h, effective hole trap density N_{eff}^h, Boltzmann constant k_B, absolute temperature T, and electron charge e):

Table 1. Parameters extracted from dynamics for nominally undoped and *Sb*-doped crystals

Parameter	Nominally undoped SPS	Antimony doped SPS
ℓ_s^h	0.25 μm	0.33 μm
ℓ_D^h	1.85 μm	1.50 μm
ℓ_D^h/ℓ_s^h	7.4	4.4
$\tau_{di}^h I$	1.0 Wms/cm^2	1.4 Wms/cm^2

It should be mentioned that $\tau_{di}^h I$ values are taken from data in Fig. 4 in the range of small K where τ_s is already K-independent, while the ratios ℓ_D^h/ℓ_s^h are extracted from the comparison of τ_s at very large and very small spatial frequencies K. The screening length ℓ_s^h in SPS:Sb is known to be dependent on the intensity of the recording beams and on sample preillumination [14]; the value shown in Table 1 is a saturated value measured at large intensities above 1 W/cm^2. (This is justified below, when discussing the results of Fig. 6(a)).

At first glance the presented data might look unexpected. The antimony doped SPS crystal usually features larger values of the gain factor compared to those of nominally undoped SPS.

Optical Materials EXPRESS

This seemingly contradicts the stronger charge screening effect in SPS:Sb, which shows a larger Debye screening length ℓ_s^h = 0.33 μm. The stronger screening really reduces the gain factor, but this reduction is overcompensated by the enhanced effective Pockels coefficient as it follows from the data in Table 1 of reference [17]. This larger effective Pockels coefficient might be the consequence of a close to perfect single-domain state for SPS:Sb, comparing to nominally undoped crystals that usually possess a considerable amount of small domains with 180° orientation of the spontaneous polarization. The estimated diffusion lengths do not differ much for these crystals, but a larger value of dielectric susceptibility (280 for SPS:Sb [16, 17] instead of 230 for nominally undoped crystal [8]) makes its characteristic response time τ_s slightly longer.

Before starting the discussion of the presented results, we would like to underline that one needs to be very careful when extracting τ_s and τ_f from the simple relationship given by Eq. (1). Apart from the two processes of the fast and slow grating formation considered here, there is in addition one more dynamic process, the self-sensitizing of the SPS:Sb sample exposed to the red He-Ne laser light [14]. The lifetime of secondary centers responsible for optical sensitizing is ≈ 14 s at ambient temperature [14], but the initial generation rate of these centers after beginning of exposure is obviously intensity dependent. For particular experimental conditions the characteristic build-up time of the compensation grating might become comparable, within the time of measurement, to the effective time of sensitizing. This may lead to wrong estimates for τ_s and even for wrong impression that τ_s changes its sign (see, e.g. Fig. 4 of Ref. 16). In addition, the influence of the sensitizing process is grating spacing dependent because the ratio τ_s/τ_f depends on the spatial frequency (see Fig. 4). While at large grating spacings the manifestation of the compensation grating is clearly visible (see Fig. 1) it becomes hardly detectable at small spacings (see, e.g., Fig. 3 of Ref. 14). All measurements described above were conducted taking into consideration this danger of misinterpretation. The data for τ_s that become unreliable in critical range of high spatial frequencies are not shown in Fig. 4.

3. Discussion

The experimental data presented above show that a distinction of SPS:Sb from nominally undoped material consists of an unusually small formation time of a compensation grating (on the order of one second and shorter), which in addition appears to be intensity dependent.

To reveal the origin of an unusual behavior of compensation grating in SPS:Sb it is necessary to consider the role of antimony in this doped material. According to EPR data [19] trivalent antimony ions substitute for divalent tin ions in the crystal lattice. They remain EPR silent when the sample is kept in the dark, i.e., with no light (or no preillumination) all antimony ions are in trivalent state. If the sample is illuminated with blue (0.44 μm, He-Cd laser) light trivalent antimony gains an electron and becomes divalent, $Sb^{3+} + e \rightarrow Sb^{2+}$ [19]. This divalent state has a limited lifetime, at room temperature it returns to the trivalent state roughly within 10-20 s as determined from the lifetime of the sensitized state in [14] and confirmed further in [20]. The recharging of the antimony ion mentioned above is possible not only with high energy quantum within a range of the fundamental absorption, it occurs also with excitation by He-Ne laser light.

With the isothermal annealing technique of photogenerated EPR active centers (Sb^{2+}) [21], the activation energy of the relaxation process $Sb^{2+} \rightarrow Sb^{3+}$ was estimated to be about 0.42 ± 0.01 eV. Taking into account that the energy of He-Ne laser light photon is equal to 1.95 eV and the bandgap of nominally undoped SPS crystal is estimated to be 2.35 eV (see, e.g., [22]), the Sb^{3+}/Sb^{2+} level can be positioned 0.42 eV below the conduction band as it is shown in Fig. 5. This can be explained by the Born-Haber cycle, as described in detail in reference [23]. It is in agreement also with the fact that even for slightly antimony doped (0.5%) SPS the absorption edge is considerably shifted to the larger wavelengths [16, 17].

The photoinduced transition of an electron from the valence band to the Sb level creates

Optical Materials EXPRESS

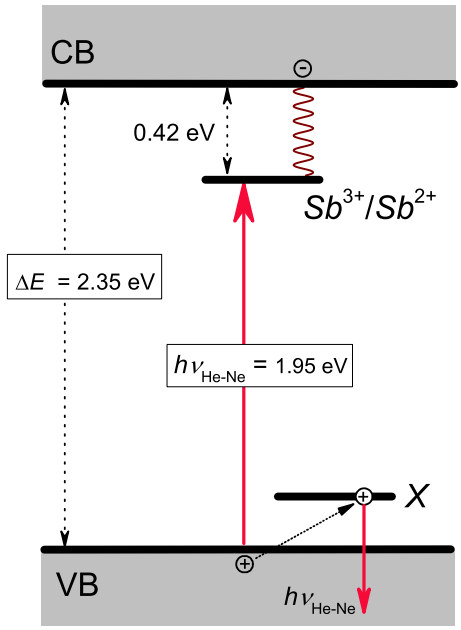

Fig. 5. Energy level diagram for antimony doped SPS. The absorption of a He-Ne laser photon creates a free hole in the valence band VB that is captured by a hole trap X and recharges the antimony ion $Sb^{3+} \rightarrow Sb^{2+}$. A portion of excessive electrons is thermally excited from the antimony level to the conduction band and thus decreases the dielectric relaxation time.

a free hole in valence band that could produce a hole polaron [24]. These hole polarons are thermally stable only at low temperatures. At ambient temperature they are quickly trapped (in sub millisecond time range) by not yet identified X-centers, which can remain positively charged much longer time but can release the holes back to VB when absorbing He-Ne light photons. These are presumably the secondary "hole donor" centers that are responsible for optical sensitizing of SPS:Sb which was discovered in [14]. A photogenerated population of positively charged X-centers increases the effective trap density, even in the case where the density of the intrinsic deep hole traps is constant and does not depend on the light intensity.

Below we consider another possible effect of the photorecharging process $Sb^{3+} \rightarrow Sb^{2+}$ that consists of creating an excessive electron density on the antimony level below the conduction band (see Fig. 5). In part, these electrons are thermally excited to the conduction band; a thermal quasiequilibrium between the antimony level and conduction band establishes at any given moment of time. Thus, the free electron density in CB should linearly follow the density of Sb^{2+} ions which, in turn, increases linearly with the light intensity. As a consequence, the electron conductivity σ^e has an intensity dependent component (with no direct optical excitation of the electrons to the conduction band); this is also true for the dielectric relaxation time $\tau^e_{di} = \epsilon\epsilon_0/\sigma^e$. In such a way the intensity dependence of a slow grating relaxation time (see Fig. 2b) is also explained. (It is quite understandable that such an intensity dependence would not exist if the lifetime of Sb^{2+} centers were smaller than τ^e_{di}; in that case the photosensitized state would vanish before the compensation grating is developed.)

The proposed explanation does not contradict the experimental data and model described in [14], which explains the optical sensitizing of SPS:Sb. A conclusion of this last paper [14] is that the effective trap density increases with the intensity of the recording light or with the time of preillumination. Following the explanation given in the present article, one can express the

Optical Materials EXPRESS

effective hole trap density for SPS:Sb as follows:

$$N^h_{eff} = \frac{\left[N^h_D(0) + \nu^h_D I\right] N^h_T}{N^h_D(0) + \nu^h_D I + N^h_T}, \tag{2}$$

where $N^h_D(0)$ and N^h_T are the densities of intrinsic hole donors and hole traps of SPS, while $\nu^h_D I$ is the density of photogenerated hole donors (i.e, the density of positively charged X-centers). It is linearly dependent on the light intensity and directly related to the presence of antimony impurity. Note that within this model $\nu^h_D I$ defines the population density of divalent antimony, because the absorption of the He-Ne laser light creates equal amounts of Sb^{2+} and positively charged X-centers.

One prediction of Eq. (2), which can be checked experimentally, is that with reasonable parameters the effective trap density N^h_{eff} should saturate with the recording light intensity even within the accepted assumption that no saturation occurs for the Sb^{2+} density itself.

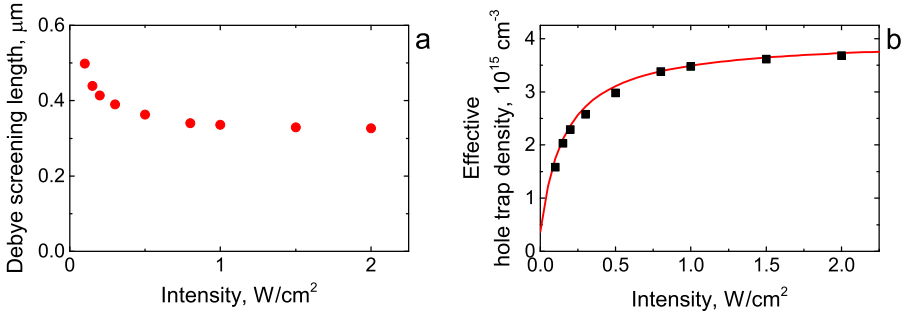

Fig. 6. Intensity dependence of (a) the Debye screening length ℓ^h_s and (b) the effective hole trap density N^h_{eff} SPS:Sb 1% (K33). The solid red line shows the best fit of Eq. (2) to the experimental data.

To verify this prediction we plotted the intensity dependence of the Debye screening length (Fig. 6(a)), extracted from measurements of angular dependences of the gain factor with different intensities of the recording light. Then, using the definition of the screening length $\ell^h_s = \sqrt{\epsilon\epsilon_0 k_B T / N^h_{eff} e^2}$, the intensity dependence of N^h_{eff} was plotted, as shown by solid squares in Fig. 6(b), with $\epsilon = 280$ [17]. The red line shows the best fit of Eq.(2) to the experimental data. The fit gives the following set of parameters

$$N^h_D(0) = 4.0 \cdot 10^{14}\, cm^{-3},$$
$$N^h_T = 4.0 \cdot 10^{15}\, cm^{-3},$$
$$\nu^h_D = 2.7 \cdot 10^{16}\, (cmW)^{-1},$$

with the accuracy that cannot exceed that of N^h_{eff} evaluation, $\Delta N/N \approx 0.05$.

In formal way the dependences shown in Fig. 6 can be explained well by the expression for N^h_{eff} with a hole trap density which is intensity dependent but the hole donors density remains constant. This explanation is, however, much less probable taking into account that the transport of positively charged species is responsible for space charge formation both in nominally undoped and antimony doped $Sn_2P_2S_6$.

As it follows from values shown above and the data from Fig. 6(b), the effective hole trap density $N^h_{eff} \approx 4.0{\cdot}10^{15}$ cm^{-3} remains moderate even when saturated at large intensities. It is smaller, for example, as compared to $N^h_{eff} \approx 2{\cdot}10^{16}$ cm^{-3} for nominally undoped $BaTiO_3$ [25] and that

Optical Materials EXPRESS

of photorefractive semiconductor CdTe (N_{eff} = 2.4·10^{16} cm^{-3} at 1.064 μm and 1.1·10^{16} cm^{-3} at 1.55 μm [26]). Finally, it is orders of magnitude smaller than in photorefractive crystals that allow for efficient recording of the reflection-type space-charge gratings, $LiNbO_3$:Fe ($N^e_{eff} \approx 10^{18}$ cm^{-3} [27]) and reduced $KNbO_3$:Fe ($N^e_{eff} \approx 10^{17}$ cm^{-3}, based on data of [23]).

It seems, for antimony doped SPS the effective trap density is presently limited by the insufficient density of the intrinsic hole traps N^h_T. One can expect a considerable improvement of two-beam coupling gain, especially at high spatial frequencies of the recorded gratings if this problem could be solved by advancements in SPS growth technologies.

Funding

This work was supported in part by European Office of Aerospace Research and Development (EOARD) via Science and Technology Center Ukraine (STCU), Project P585a.

Acknowledgments

We are grateful to A. Grabar and I. Stoyka for SPS crystals.